

# Structural Insights and the Surprisingly Low Mechanical Stability of the Au–S Bond in the Gold-Specific Protein GolB

Wei Wei,<sup>†,‡,#</sup> Yang Sun,<sup>§,#</sup> Mingli Zhu,<sup>†,‡</sup> Xiangzhi Liu,<sup>†,‡</sup> Peiqing Sun,<sup>†,‡</sup> Feng Wang,<sup>||</sup> Qiu Gui,<sup>‡</sup> Wuyi Meng,<sup>||</sup> Yi Cao,<sup>\*,§</sup> and Jing Zhao<sup>\*,†,‡</sup>

<sup>†</sup>State Key Laboratory of Coordination Chemistry, Institute of Chemistry and BioMedical Sciences, School of Chemistry and Chemical Engineering, Collaborative Innovation Center of Chemistry for Life Sciences, <sup>‡</sup>State Key Laboratory of Pharmaceutical Biotechnology, School of Life Sciences, and <sup>§</sup>Collaborative Innovation Center of Advanced Microstructures, National Laboratory of Solid State Microstructure, Department of Physics, Nanjing University, Nanjing 210093, China

<sup>||</sup>Elias James Corey Institute of Biomedical Research, Wuxi Biortus Biosciences Co., Ltd, Jiangyin, 214437, China

**S** Supporting Information

**ABSTRACT:** The coordination bond between gold and sulfur (Au–S) has been widely studied and utilized in many fields. However, detailed investigations on the basic nature of this bond are still lacking. A gold-specific binding protein, GolB, was recently identified, providing a unique opportunity for the study of the Au–S bond at the molecular level. We probed the mechanical strength of the gold–sulfur bond in GolB using single-molecule force spectroscopy. We measured the rupture force of the Au–S bond to be 165 pN, much lower than Au–S bonds measured on different gold surfaces (~1000 pN). We further solved the structures of apo-GolB and Au(I)–GolB complex using X-ray crystallography. These structures showed that the average Au–S bond length in GolB is much longer than the reported average value of Au–S bonds. Our results highlight the dramatic influence of the unique biological environment on the stability and strength of metal coordination bonds in proteins.

Gold–thiol interactions have been widely used in materials science, molecular biology, and medical engineering. Their versatile applications include self-assembled monolayers (SAM) of bio- or organic molecules on gold, biosensing, drug delivery, and gold nanoparticle catalysis.<sup>1–4</sup> The covalent bond between gold and sulfur (Au–S) provides a robust and modifiable linkage that is key to the nanostructures between the gold surface and the thiol-containing molecules.<sup>5</sup> To probe the detailed nature of gold–thiol interactions, Gaub et al. have performed pioneering work to detect the strength of a single Au–S bond, using atomic force microscopy (AFM)-based single-molecule force spectroscopy (SMFS).<sup>6</sup> The structural details and the strength of the Au–S bond in gold–thiol interactions are attracting great attention recently.<sup>7</sup> Encouragingly, Zhang et al. successfully employed the AFM-based SMFS method to quantify the strength of individual thiol–gold bonds with different gold surface properties and sample preparation conditions<sup>8</sup> (Figure 1A). These results suggested that the strength of thiol–gold bonds in self-assembled monolayers depended largely on the chemical environment that are difficult to define.

Numerous metalloproteins, including transcription regulators and metallochaperones, are involved in maintaining the delicate

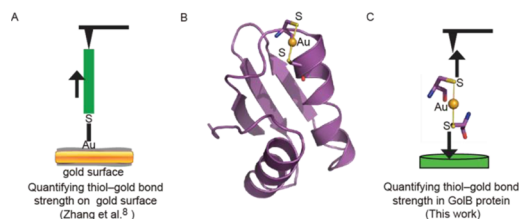


**Figure 1.** (A) Illustration of the breakage of an isolated Au–S bond on the material’s surface (Zhang et al.). (B) Crystal structure of Au(I)-bound GolB protein. (C) Illustration of the breakage of an Au–S bond in Au(I)-bound GolB protein (this work).

homeostasis of cellular concentrations of various metal ions in bacteria.<sup>9–14</sup> Recently, it was discovered that several proteins can bind gold ions and form the Au–S bond selectively.<sup>15–18</sup> Our previous research on wide-type GolB protein from *Salmonella typhimurium* showed that GolB binds Au(I) using a conserved Cys-XX-Cys binding domain and with a much higher affinity than Cu(I).<sup>16</sup> In gold sensing and resistant bacteria, the *gol* regulon including GolB was regulated by Au(I) and involved with Au-homeostasis *in vivo*.<sup>15,19</sup> In this detoxification process, GolB is in charge of binding excessive free gold ions from cytoplasm and/or periplasm.<sup>19</sup> Thus, the Au–S bonds in GolB must be generated and broken in a more dynamic process for releasing gold ions than that in nonprotein gold complexes. Exploring the mechanical stability of Au–S bonds in single-protein settings may provide insights into the structure–function relationship of metalloproteins. However, the structural details of gold coordination and data on the stability of Au–S bonds in GolB are lacking.

Interestingly, Zheng and Li elegantly demonstrated that the mechanical strength of Fe–S bonds is extremely sensitive to the chemical and biological environment of the proteins.<sup>20–24</sup> Because Au–S bonds are generally considered to be covalent bonds and are much stronger than Fe–S coordination bonds, we are intrigued to see how the protein environment could affect the mechanical stability of Au–S bonds.

Here, combining X-ray crystallography and the AFM-based SMFS methods, we studied the structural and mechanical

Received: September 20, 2015

Published: November 13, 2015

properties of Au–S bonds in a metalloprotein for the first time (Figure 1B,C). We discovered that the Au–S bonds in GolB are unusually longer than those in their inorganic counterparts. They are also longer than the Au–S bond (2.32 and 2.39 Å) found in the Cu metalloregulatory protein, CueR.<sup>13</sup> The mechanical stability of Au–S bonds in GolB was much lower than that of typical covalent bonds. Our results highlight the importance of protein environment on the stability and dynamics of Au–S bonds in single-molecule settings.

We used the AFM-based SMFS method to directly rupture single Au–S bonds in GolB and probe their mechanical properties. To unambiguously identify single-molecule stretching events, we prepared a chimeric polyprotein (GB1-GolB)<sub>4</sub> (Figure 2A, inset). The well-characterized GB1 was used as a

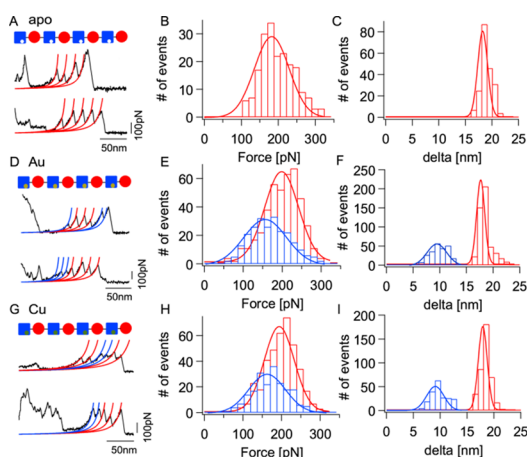


**Figure 2.** SMFS experiments on GolB in the absence and presence of Au or Cu. To probe the mechanical stability of Au–S and Cu–S bonds in GolB (colored in blue), we engineered a polyprotein ( $\beta$ -GB1-GolB)<sub>4</sub> (insets in A, D, and G) in which GB1 (colored in red) is used to provide a “mechanical fingerprint” for single-molecule events. A  $\beta$ -hairpin of  $\sim 9$  nm was inserted between the -CXXC- metal binding motif of GolB to provide sufficient contour length increments for recognition of the rupture of Au–S or Cu–S bonds in the force–extension traces. The representative force–extension traces, unfolding force histogram, and distribution of contour length increments for the stretching of ( $\beta$ -GB1-GolB)<sub>4</sub> in the apo form are shown in A, B, and C, respectively. No unfolding events of apo-GolB were observed, owing to its low mechanical stability. The representative force–extension traces, unfolding force histogram, and distribution of contour length increments for the stretching of ( $\beta$ -GB1-GolB)<sub>4</sub> charged with Au are shown in D, E, and F, respectively. The peaks with contour length increments of  $\sim 9$  nm are assigned as the rupture events of Au–S bonds. The representative force–extension traces, unfolding force histogram, and distribution of contour length increments for the stretching of ( $\beta$ -GB1-GolB)<sub>4</sub> charged with Cu are shown in G, H, and I, respectively.

basis to identify the rupture events of GolB. The loop between the two gold-binding cysteine residues in GolB is too short to provide sufficient distance change for AFM to detect after the rupture of Au–S bonds. Therefore, we inserted a fast-folding  $\beta$ -hairpin into the gold binding motif of GolB, following similar protocols introduced by others.<sup>22,25,26</sup> The chimeric polyprotein using the GolB with inserted  $\beta$ -hairpin referred as ( $\beta$ -GB1-GolB)<sub>4</sub> hereafter. According to references, because the N- and C-termini of the fast-folding  $\beta$ -hairpin are very close, insertion of this  $\beta$ -hairpin does not affect the structure of engineered metalloproteins or their metal center.<sup>22,27</sup> Au(I) loading experiments<sup>17,28</sup> and circular dichroism (CD) spectra also implies that the overall secondary structure of GolB did not

change with the insertion of the  $\beta$ -hairpin (Figure S1). In single-molecule AFM experiments, ( $\beta$ -GB1-GolB)<sub>4</sub> was randomly chosen from a glass surface with an AFM cantilever tip and stretched in PBS buffer containing 2 mM (2-carboxyethyl)-phosphine (TCEP) in the absence of gold ions. Because the attaching points of the polyprotein are uncontrolled, the number of protein domains being unfolded varies in different traces. Stretching ( $\beta$ -GB1-GolB)<sub>4</sub> results in force–extension curves that are characterized by a featureless long spacer followed by the characteristic unfolding peaks of GB1 (unfolding forces  $\sim 180$  pN and  $\Delta L_c$  of  $\sim 18$  nm).<sup>27,29,30</sup> Because GolB alternates with GB1 in the polyprotein, the long, featureless spacer preceding GB1 unfolding events must result from the stretching and unfolding of GolB. Such long, featureless spacers indicate that GolB unfolds at forces that are below the detection limit of our AFM ( $\sim 10$  pN). The distributions of the unfolding forces and contour length increments for GB1 are shown in Figure 2B,C, respectively. Then, we stretched the same polyprotein charged with gold ions. In addition to the presence of unfolding events of GB1, we observed the force peaks with  $\Delta L_c$  value of  $\sim 9$  nm (Figure 2D). Because the  $\beta$ -hairpin inserted into GolB has 15 amino acids, corresponding to a contour length of  $\sim 9$  nm, we conclude that these force peaks resulted from the rupture of Au–S bonds in GolB. The ratio between the events from the rupture of Au–S bonds and those from GB1 unfolding suggests that  $\sim 50\%$  of GolB was bound with gold ions under experimental conditions (Figure 2E,F). Surprisingly, we found that the forces of these peaks are similar to the unfolding forces of GB1, indicating low mechanical stability for such a coordination bond. The distribution of the rupture forces of the Au–S bonds in GolB is shown in Figure 2E. The average forces are  $165 \pm 55$  pN, which are significantly lower than the mechanical stability of Au–S bonds from other nonprotein gold complexes ( $\sim 0.5$ – $1$  nN).<sup>8</sup> Interestingly, the rupture forces are similar to those of Fe–S bonds in rubredoxin.<sup>34</sup> This provides additional evidence that the strength of the coordinate bonds can be dramatically modulated by the protein environment. We further studied the Cu–S bond in GolB when the protein is charged by copper ions. Similarly, we observed force peaks with contour length increments of  $\sim 9$  nm for the rupture of Cu–S bonds in addition to the unfolding events for GB1 (Figure 2G). Interestingly, the rupture forces for Cu–S are comparable with those for the Au–S bond in GolB, while there is a significant difference in binding affinity between GolB to Au and Cu.<sup>16</sup> Notably, the observed rupture events for Cu–S bonds are around 52% of the unfolding events for GB1 (Figure 2H,I), comparable with the Au–S bonds (50%). The bond strength for Au–S and Cu–S is much less than that for disulfide bonds with rupture forces more than 450 pN under the same condition (Figure S2).<sup>31</sup> Therefore, we hypothesize that the protein environment of GolB plays a major role in modulating the mechanical stability of the metal–thiol bonds.

To further understand the weak mechanical strength of the Au–S bond in GolB at the atomic level, we solved the crystal structures of GolB proteins in different states, including oxidized/reduced GolB and Au(I)–GolB complex. First, gold ions were used as the heavy atom derivative to solve the phase by the single wavelength anomalous dispersion (SAD) method, and the oxidized apo-GolB structure was obtained at a 1.40 Å resolution. The structure of oxidized apo-GolB showed that the two cysteines (Cys<sup>10</sup> and Cys<sup>13</sup>) in the CXXC domain formed a disulfide bond without Au(I) binding (Figure 3A), even in the heavy atom derivative structure. Next, treatment of the reductive TCEP resulted in a reduced apo-GolB structure with a 1.80 Å

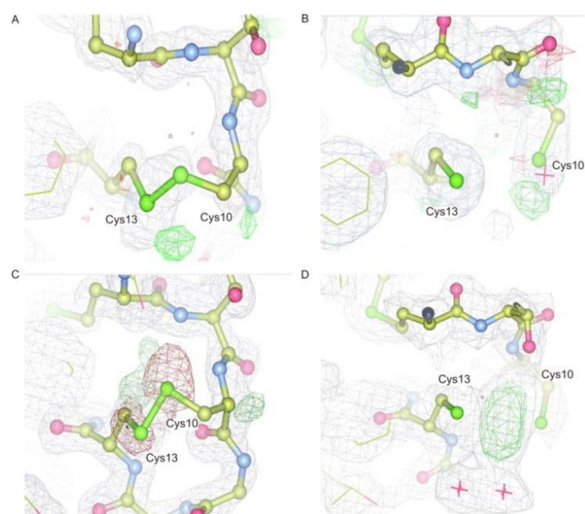


**Figure 3.** Stereo view of  $2F_o - F_c$  electron density map (light gray, contoured at  $1.00\sigma$ ) at the metal binding site in the GolB X-ray structure. (A) Au(I)- and (B) TCEP-soaked structures. (C) The negative density demonstration in the TCEP-soaked structure. (D) Au(I)- and TCEP-soaked structures (green, contoured at  $9\sigma$ ).

resolution where the disulfide bond between Cys<sup>10</sup> and Cys<sup>13</sup> was broken (Figure 3B). The negative density in Figure 3C confirmed that there was no disulfide bond formed between the two cysteines in the reduced form of apo-GolB. Last, in the sequential soaked structure of TCEP and Au(I), the gold atom was found between Cys<sup>10</sup> and Cys<sup>13</sup>, forming two coordination bonds as shown in Figure 3D.

At 1.80 Å resolution, the Cys<sup>10</sup> C $\alpha$  atom in the reduced form of apo-GolB moved away from its position in the oxidized form, with a distance of 4.79 Å. In contrast, the Cys<sup>13</sup> C $\alpha$  atom stayed in the rigid helix area ( $\alpha 1$ ), most likely to open an appropriate space for metal ions participating in a disulfide bond with Cys<sup>13</sup> (Figure 4A,B). This shift changes the position of the metal binding loop between residues 10 and 13, while the rest of the structure is unaltered. Furthermore, the structure of Au(I)-bound GolB was determined at 2.00 Å resolution (PDB accession code: 4Y2I), with a measured distance of two sulfur atoms at 5.09 Å. Compared to the reduced apo-GolB structure, it shows little conformational changes except the metal binding domain (Figure 4C). The coordinate-covalent Au–S bonds reveal a bond angle of 172.48°, which is similar to reported S–Au(I)–S linear coordination<sup>32</sup> (Figure 4D). The average Au–S bond length (2.55 Å) is much longer than the reported average value (~2.40 Å).<sup>13,33</sup> It is worth noting that because the Au binding motif is located on the N-terminus of an  $\alpha$  helix, the two Au-binding thiolates are surrounded by positively charged backbone NH groups. The favorable interaction between the cysteines with helix dipole could greatly lower the coordination capability of the sulfide. Especially, the backbone NH from amino acid Gly<sup>11</sup> is only 3.03 Å away from Cys<sup>10</sup> thiolate (Figure 4D), which could potentially form hydrogen bonds with the thiolate. The charge–charge interaction and hydrogen bonding among them could greatly neutralize the charge of thiolate and thus weaken the Au–S bonds.<sup>13</sup>

The structure–property relationship of a chemical bond is of fundamental importance in science. However, most studies have focused mainly on chemical bonds in simple chemical environments. Here we show that in single-molecule settings, the properties of a chemical bond can be significantly modulated.

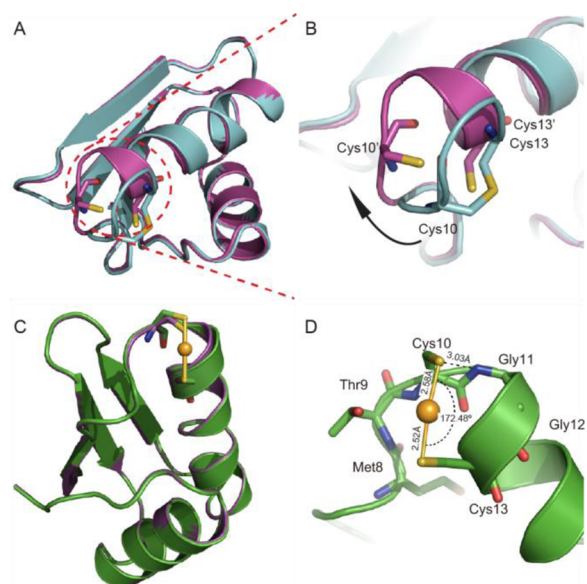


**Figure 4.** (A) Superposition of the overall structures of oxidized apo-GolB (cyan, PDB accession code: 4Y2M) and reduced apo-GolB (magenta, PDB accession code: 4Y2K). (B) Close-up view of the Cys<sup>10</sup> shift between oxidized apo-GolB and reduced apo-GolB. (C) Superposition of the overall structures of reduced apo-GolB (magenta) and Au(I)-bound GolB (green). (D) Close-up view detailing the Au(I)–S coordinate-covalent bonds and hydrogen-bonding interactions at the GolB metal-binding pocket.

Generally believed that highly covalent and strong Au–S bonds are much weaker in a protein than those on a nonprotein surface.<sup>6–8</sup> It is worth mentioning that the chemical environment on gold surfaces is poor understood. This could lead to dramatically different mechanical strength of Au–S bonds.<sup>8</sup> Currently, it is still technically difficult to study the mechanical strength of Au–S bonds in well-defined inorganic complexes. Although the protein environment is also complex, it is well-defined and can be further understood through X-ray crystallography. Therefore, the protein system provides us tremendous possibilities to understand the fundamental metal–thiol binding in details. The mechanical stability of Au–S bond in GolB is comparable to many noncovalent interactions, including the rupture of streptavidin–biotin interaction and protein unfolding. Similarly, Zheng and Li demonstrated that the Fe–S and Zn–S bonds of high covalency in a protein environment are also mechanically weak (Table 1).<sup>24,34</sup> Moreover, two inspiring reports from the Garcia-Manyes

**Table 1. Strengths of Single Metal–Thiol Bonds in Protein or Nonprotein Surfaces**

single thiol–metal bond	strength (pN)		ref
	protein	nonprotein	
Au–S	165 ± 55		this work
		1400 ± 300	6
		2200–2900	7
		500–1000	8
Cu–S	171 ± 47	NA	this work
		~45	33
Zn–S	~170	NA	31
		~90	32
Fe–S	~211	300–500	23

group, respectively, showed that the mechanical lability of the individual Zn–S bonds in zinc finger was only ~90 pN and the rupture forces of Cu–S bonds in plastocyanin and azurin are only ~45 pN.<sup>15,35</sup> The strength of the metal coordination bonds could be precisely tailored in protein environments through evolution for specific biological functions. The combination of X-ray crystallography and SMFS provides a unique way to probe the underlying mechanism.

Based on our results, the low mechanical stability of Au–S bonds in GolB may originate from the following two major aspects. First, the low mechanical stability of Au–S bonds in GolB might be associated with the chemical environment around the Au–S bonds in the protein. As revealed by the crystal structure, GolB exhibits a classic  $\beta\alpha\beta\beta\beta$ -fold structure similar to that observed for other homologues.<sup>36,37</sup> Two Au-binding thiolates from Cys<sup>10</sup> and Cys<sup>13</sup> are surrounded by backbone NH groups of residues 8–13 in a range of ~3–4 Å. As well documented in literature,<sup>38,39</sup> such a positively charged environment around the N terminus of a helix dipole could potentially neutralize the charges on the thiolates by direct charge–charge interactions. Moreover, the hydrogen bonding could further weaken the chelation capability of the thiolates, leading to weakened Au–S bonds.<sup>13</sup> Second, the length of Au–S bonds in GolB is much longer than those in inorganic complexes; hence, the Au–S bond in GolB bond is intrinsically weaker.

Our finding that the Au–S bonds in GolB are mechanically weak may be valuable for the understanding of the biological function of GolB protein. According to previous research on the gold sensing and resistance function of *Salmonella gol* regulons, GolB protein expression is regulated by GolS under gold ion induction.<sup>19</sup> It was proposed that GolB needs to competitively bind toxic gold ions with a high affinity, while not affecting the function of other copper trafficking proteins. Additionally, GolB also must deliver gold ions to the P-type ATPase GolT, which functions as gold transporter. Thus, the combination of high gold binding affinity and mechanically weak Au–S bonds allows GolB to robustly sustain the biological function as a gold chaperone, which might suggest a general principle for the trafficking of metal ions *in vivo*.

## ■ ASSOCIATED CONTENT

### Supporting Information

The Supporting Information is available free of charge on the ACS Publications website at DOI: 10.1021/jacs.5b09895.

Experimental details and crystallographic data. The structure has been deposited in the Protein Data Bank as entry 4Y2M, 4Y2K, 4Y2I (PDF)

## ■ AUTHOR INFORMATION

### Corresponding Authors

\*caoyi@nju.edu.cn

\*jingzhao@nju.edu.cn

### Author Contributions

<sup>#</sup>These authors contributed equally to this work.

### Notes

The authors declare no competing financial interest.

## ■ ACKNOWLEDGMENTS

Financial support was provided by the Doctoral Fund of the Ministry of Education of China, the Guangdong Government (S20120011226), the National Science Foundation of China

(21332005, 21571098, 31170813 and 31200607), and the MOST of China (2014AA020512).

## ■ REFERENCES

- (1) Love, J. C.; Estroff, L. A.; Kriebel, J. K.; Nuzzo, R. G.; Whitesides, G. M. *Chem. Rev.* **2005**, *105*, 1103.
- (2) Boisselier, E.; Astruc, D. *Chem. Soc. Rev.* **2009**, *38*, 1759.
- (3) Vericat, C.; Vela, M. E.; Benitez, G.; Carro, P.; Salvarezza, R. C. *Chem. Soc. Rev.* **2010**, *39*, 1805.
- (4) Giljohann, D. A.; Seferos, D. S.; Daniel, W. L.; Massich, M. D.; Patel, P. C.; Mirkin, C. A. *Angew. Chem., Int. Ed.* **2010**, *49*, 3280.
- (5) Hakkinen, H. *Nat. Chem.* **2012**, *4*, 443.
- (6) Grandbois, M.; Beyer, M.; Rief, M.; Clausen-Schaumann, H.; Gaub, H. E. *Science* **1999**, *283*, 1727.
- (7) Hollinger, M. A. *Crit. Rev. Toxicol.* **1996**, *26*, 255.
- (8) Xue, Y.; Li, X.; Li, H.; Zhang, W. *Nat. Commun.* **2014**, *5*.
- (9) O'Halloran, T.; Walsh, C. *Science* **1987**, *235*, 211.
- (10) Finney, L. A.; O'Halloran, T. V. *Science* **2003**, *300*, 931.
- (11) Borremans, B.; Hobman, J. L.; Provoost, A.; Brown, N. L.; van der Lelie, D. *J. Bacteriol.* **2001**, *183*, 5651.
- (12) Brown, N. L.; Stoyanov, J. V.; Kidd, S. P.; Hobman, J. L. *Fems Microbiol. Rev.* **2003**, *27*, 145.
- (13) Changela, A.; Chen, K.; Xue, Y.; Holschen, J.; Outten, C. E.; O'Halloran, T. V.; Mondragón, A. *Science* **2003**, *301*, 1383.
- (14) Hobman, J. L. *Mol. Microbiol.* **2007**, *63*, 1275.
- (15) Checa, S. K.; Espariz, M.; Perez Audero, M. E.; Botta, P. E.; Spinelli, S. V.; Soncini, F. C. *Mol. Microbiol.* **2007**, *63*, 1307.
- (16) Wei, W.; Zhu, T. Z.; Wang, Y.; Yang, H. L.; Hao, Z. Y.; Chen, P. R.; Zhao, J. *Chem. Sci.* **2012**, *3*, 1780.
- (17) Jian, X.; Wasinger, E. C.; Lockard, J. V.; Chen, L. X.; He, C. *J. Am. Chem. Soc.* **2009**, *131*, 10869.
- (18) Pontel, L. B.; Audero, M. E. P.; Espariz, M.; Checa, S. K.; Soncini, F. C. *Mol. Microbiol.* **2007**, *66*, 814.
- (19) Checa, S. K.; Soncini, F. C. *BioMetals* **2011**, *24*, 419.
- (20) Gupta, A.; Matsui, K.; Lo, J. F.; Silver, S. *Nat. Med.* **1999**, *5*, 183.
- (21) Lee, J.; Peña, M. M. O.; Nose, Y.; Thiele, D. J. *J. Biol. Chem.* **2002**, *277*, 4380.
- (22) Zheng, P.; Takayama, S.-i. J.; Mauk, A. G.; Li, H. *J. Am. Chem. Soc.* **2013**, *135*, 7992.
- (23) Chernousova, S.; Epple, M. *Angew. Chem., Int. Ed.* **2013**, *52*, 1636.
- (24) Zheng, P.; Li, H. B. *J. Am. Chem. Soc.* **2011**, *133*, 6791.
- (25) Su, C. C.; Long, F.; Yu, E. W. *Protein Sci.* **2011**, *20*, 6.
- (26) Gitschier, J.; Moffat, B.; Reilly, D.; Wood, W. L.; Fairbrother, W. J. *Nat. Struct. Biol.* **1998**, *5*, 47.
- (27) Cao, Y.; Li, H. *Nat. Mater.* **2007**, *6*, 109.
- (28) Wei, W.; Zhu, T.; Wang, Y.; Yang, H.; Hao, Z.; Chen, P. R.; Zhao, J. *Chem. Sci.* **2012**, *3*, 1780.
- (29) Banci, L.; Bertini, I.; Cantini, F.; Chasapis, C. T.; Hadjilias, N.; Rosato, A. *J. Biol. Chem.* **2005**, *280*, 38259.
- (30) Hamza, I.; Schaefer, M.; Klomp, L. W. J.; Gitlin, J. D. P. *Proc. Natl. Acad. Sci. U. S. A.* **1999**, *96*, 13363.
- (31) Ainavarapu, S. R. K.; Bruić, J.; Huang, H. H.; Wiita, A. P.; Lu, H.; Li, L.; Walther, K. A.; Carrion-Vazquez, M.; Li, H.; Fernandez, J. M. *Biophys. J.* **2007**, *92*, 225.
- (32) Shaw, C. F. *Chem. Rev.* **1999**, *99*, 2589.
- (33) Gronbeck, H.; Walter, M.; Hakkinen, H. *J. Am. Chem. Soc.* **2006**, *128*, 10268.
- (34) Zheng, P.; Li, H. B. *Biophys. J.* **2011**, *101*, 1467.
- (35) Ratte, H. T. *Environ. Toxicol. Chem.* **1999**, *18*, 89.
- (36) Wernimont, A. K.; Huffman, D. L.; Lamb, A. L.; O'Halloran, T. V.; Rosenzweig, A. C. *Nat. Struct. Biol.* **2000**, *7*, 766.
- (37) Boal, A. K.; Rosenzweig, A. C. *Chem. Rev.* **2009**, *109*, 4760.
- (38) Hol, W. G. J.; van Duijnen, P. T.; Berendsen, H. J. C. *Nature* **1978**, *273*, 443.
- (39) Aqvist, J.; Luecke, H.; Quioco, F. A.; Warshel, A. P. *Proc. Natl. Acad. Sci. U. S. A.* **1991**, *88*, 2026.